PLASMOID MERGER AND SHOCK WAVE DURING THE MAGNETIC RECONNECTION ON THE ACCRETION DISK OF THE SGR A*

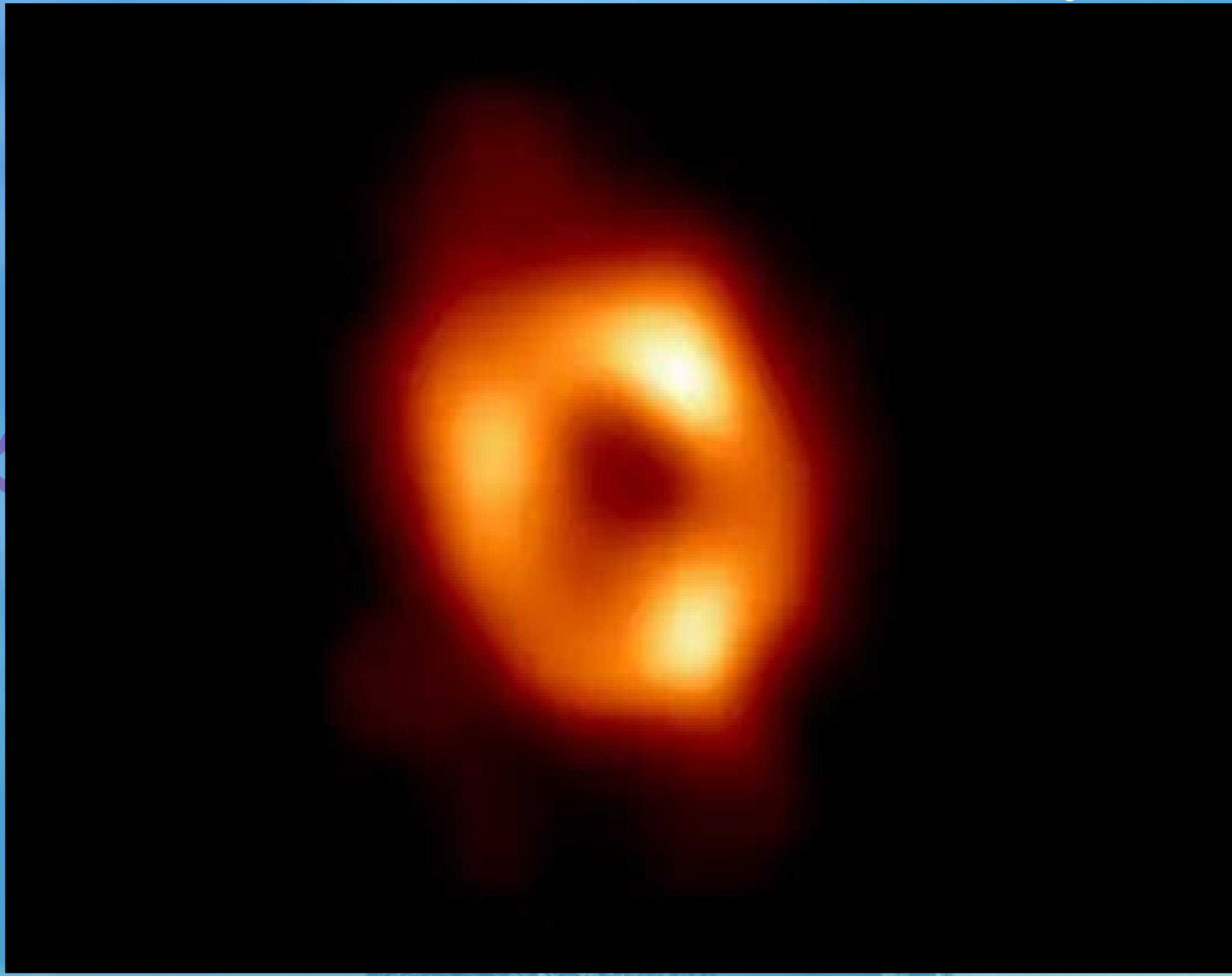

Reporter: TianLe Zhao

Co-author: YeFei Yuan, XiaoFeng Li, ZeYuan Tang, Rajiv Kumar

Outline

- Background
- Plasmoid merger during the magnetic reconnection
- Shock wave during the magnetic reconnection
- Conclusion

Background: near-infrared superflares

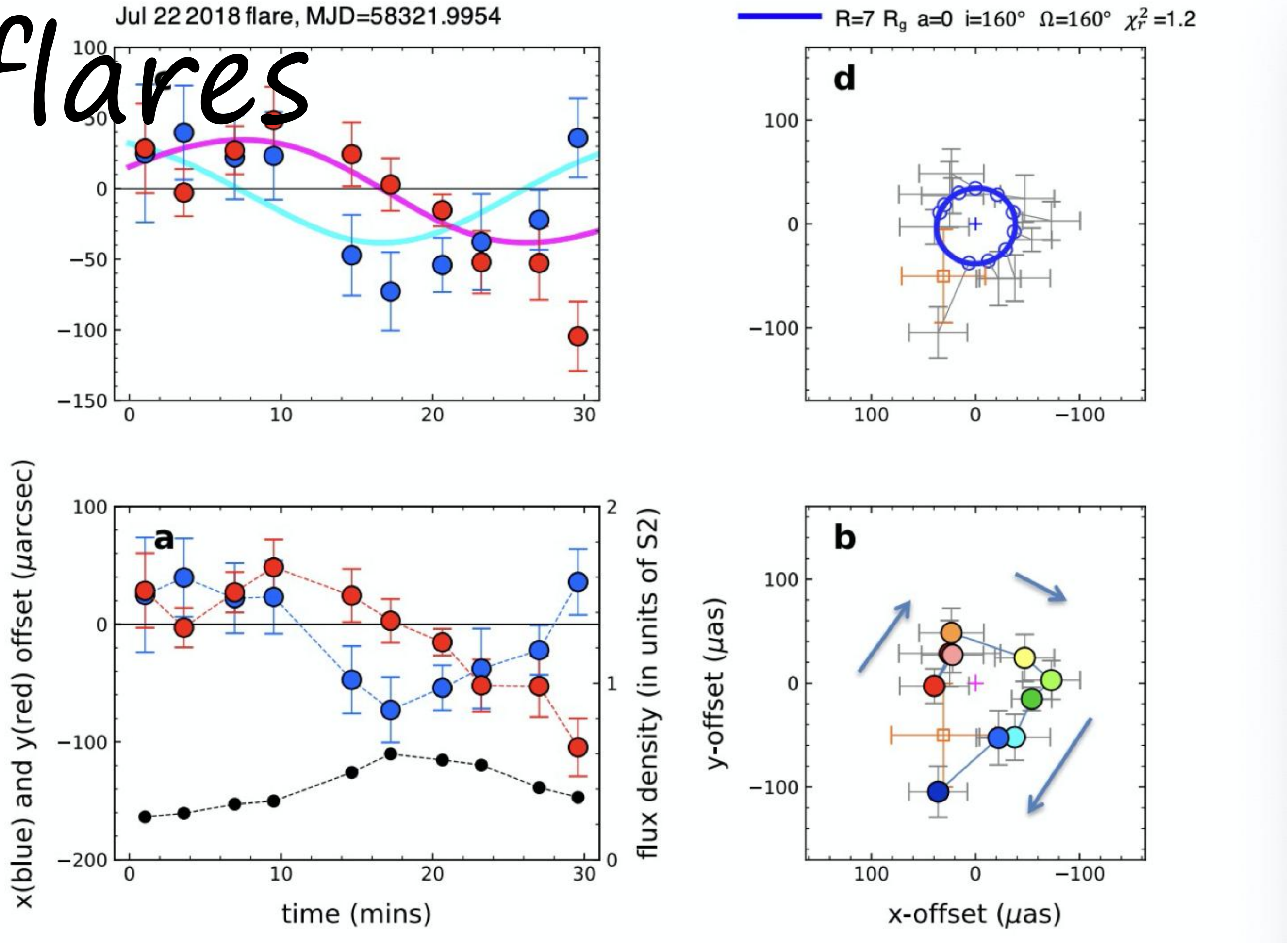

GRAVITY Collaboration+2018

Recently, VLTI observed several near-infrared superflares which might be from the hot spots at about near the blackhole from Sgr A* . It is believed that these hot spots are likely due to the relativistic magnetic reconnection event

3D numerical simulation of the flares

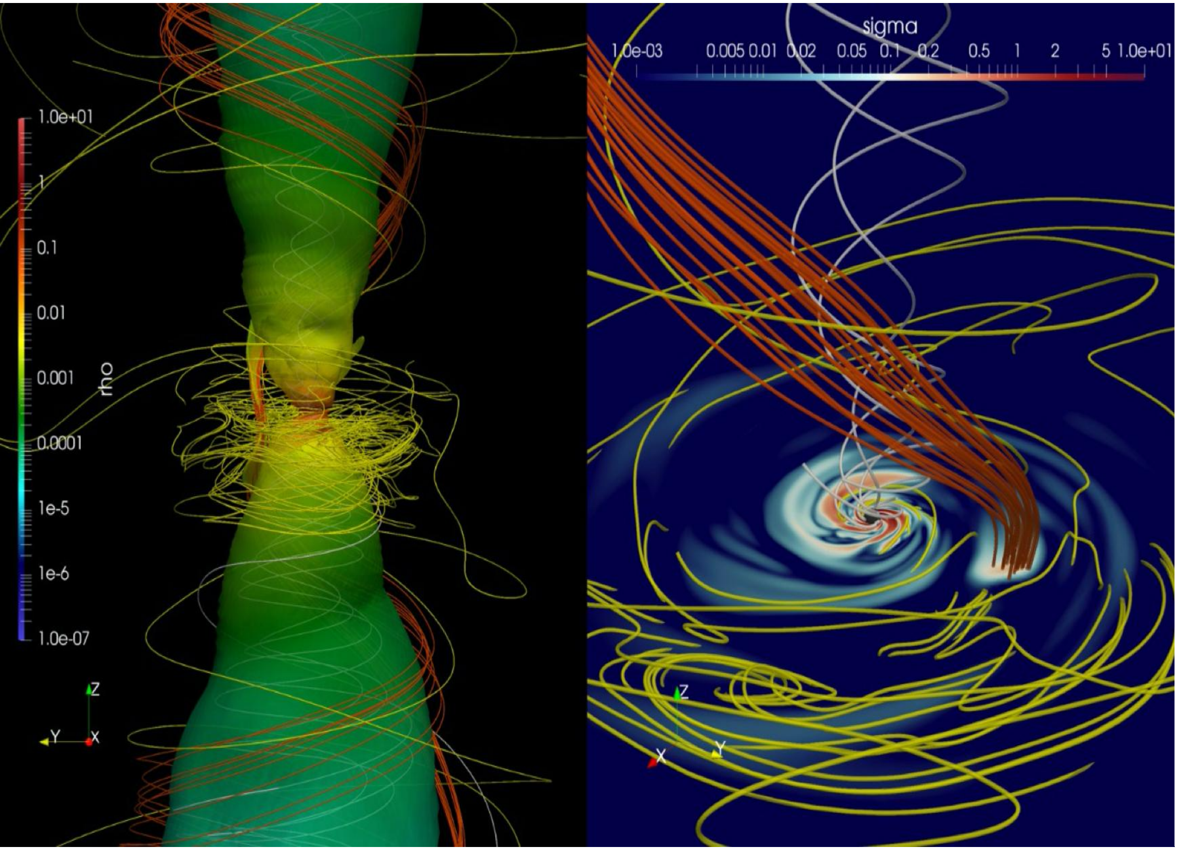

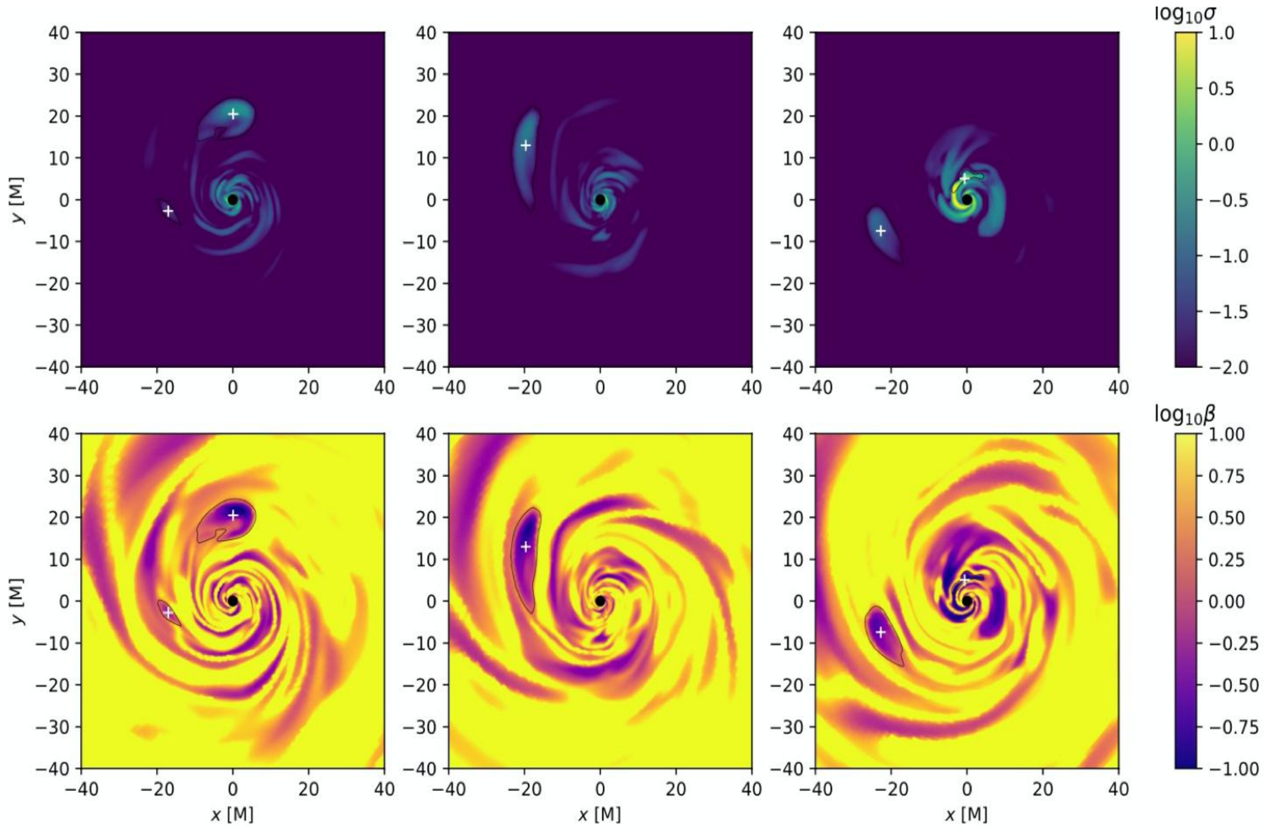

Porth et al.2020 studied a model of the flares by the 3D RMHD simulations of magnetically arrested accretion disk(MADs) and found that the magnetic reconnection in the flares event can causes particles to heat up or accelerate.

Light curve fitting of the flares

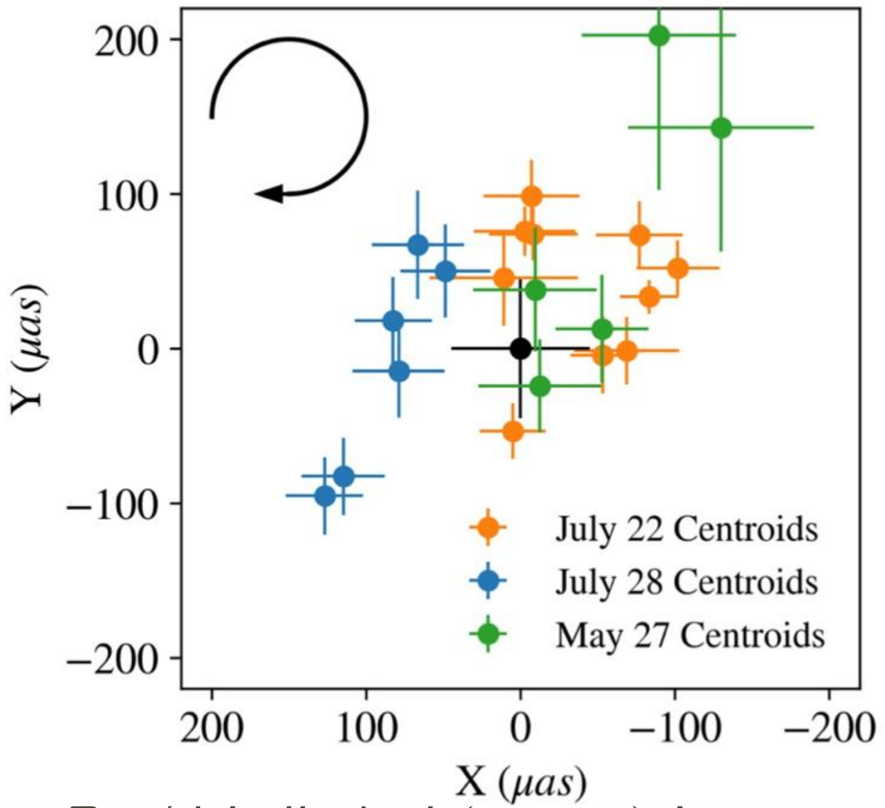

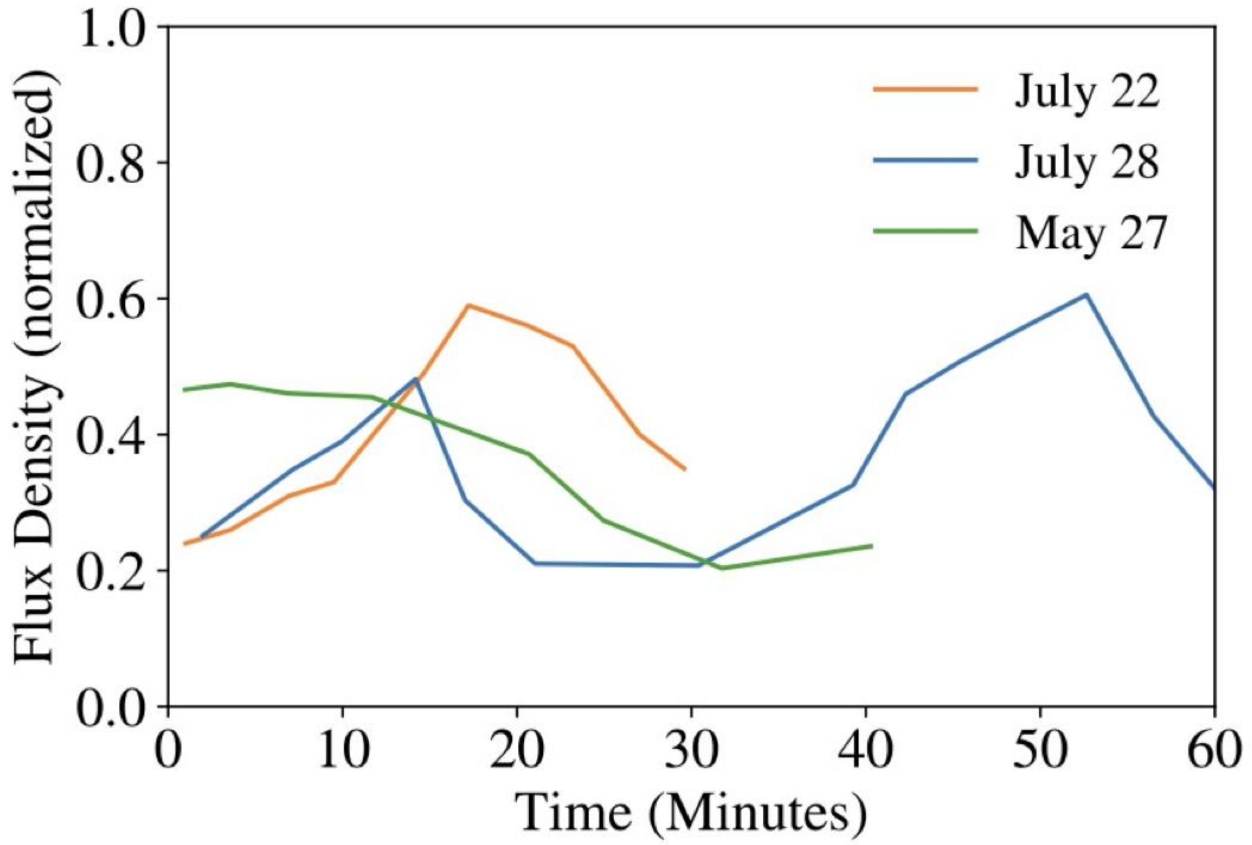

David ball et al（2020）have used th
calculations with including effects from finite plasmoid motion, particle acceleration, and synchrotron cooling obtained a flare light curves, which explained the reason that some flares has double peak or only a single peak and uncovers a connection between the structure in the light curve and the location of the flare.

3D numerical simulation of the flares

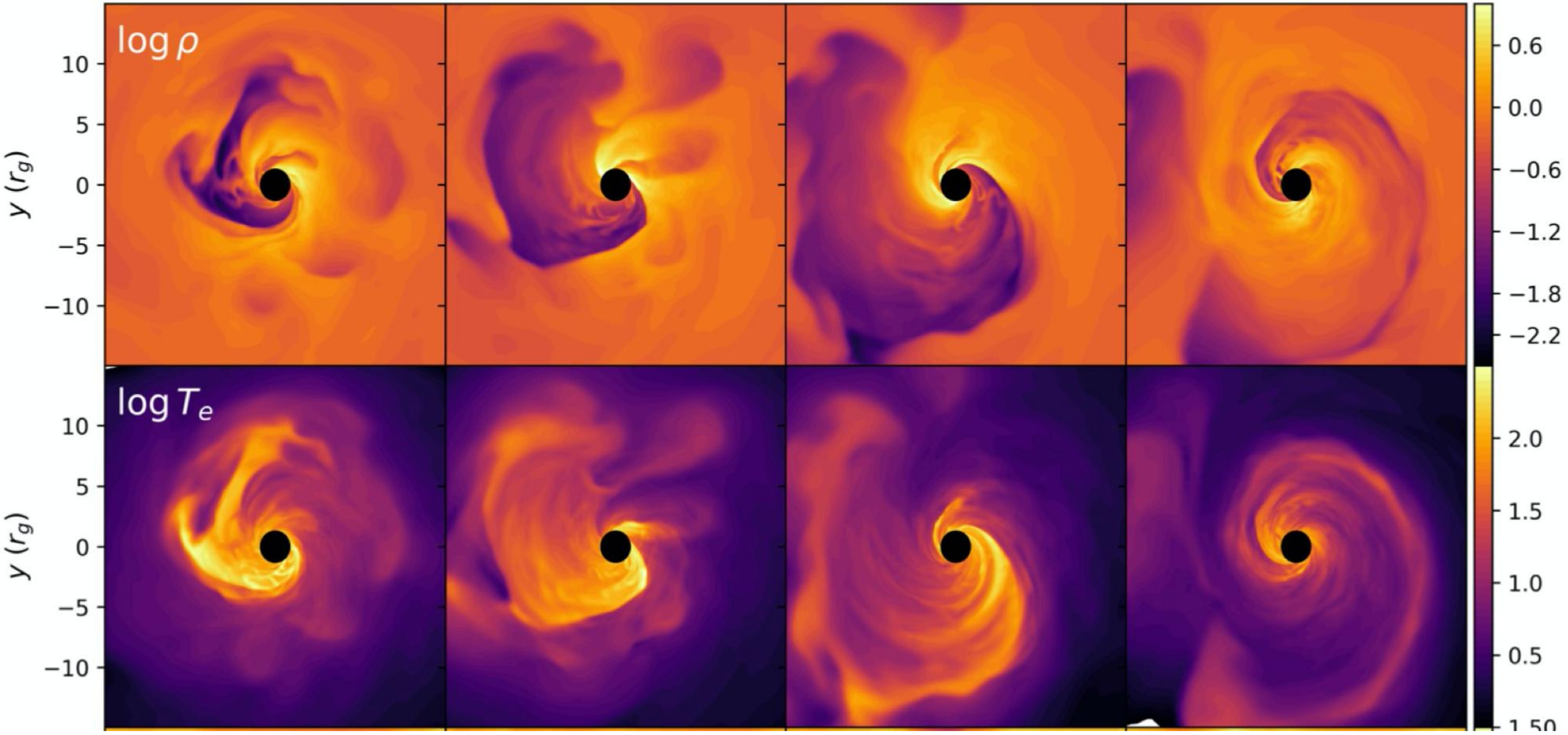

Dexter et al(2020) have studied a sample flares event observable in the near-infrared showed that the emission morphology traces the boundary of the magnetically controlled region.

Numerical simulation of flares

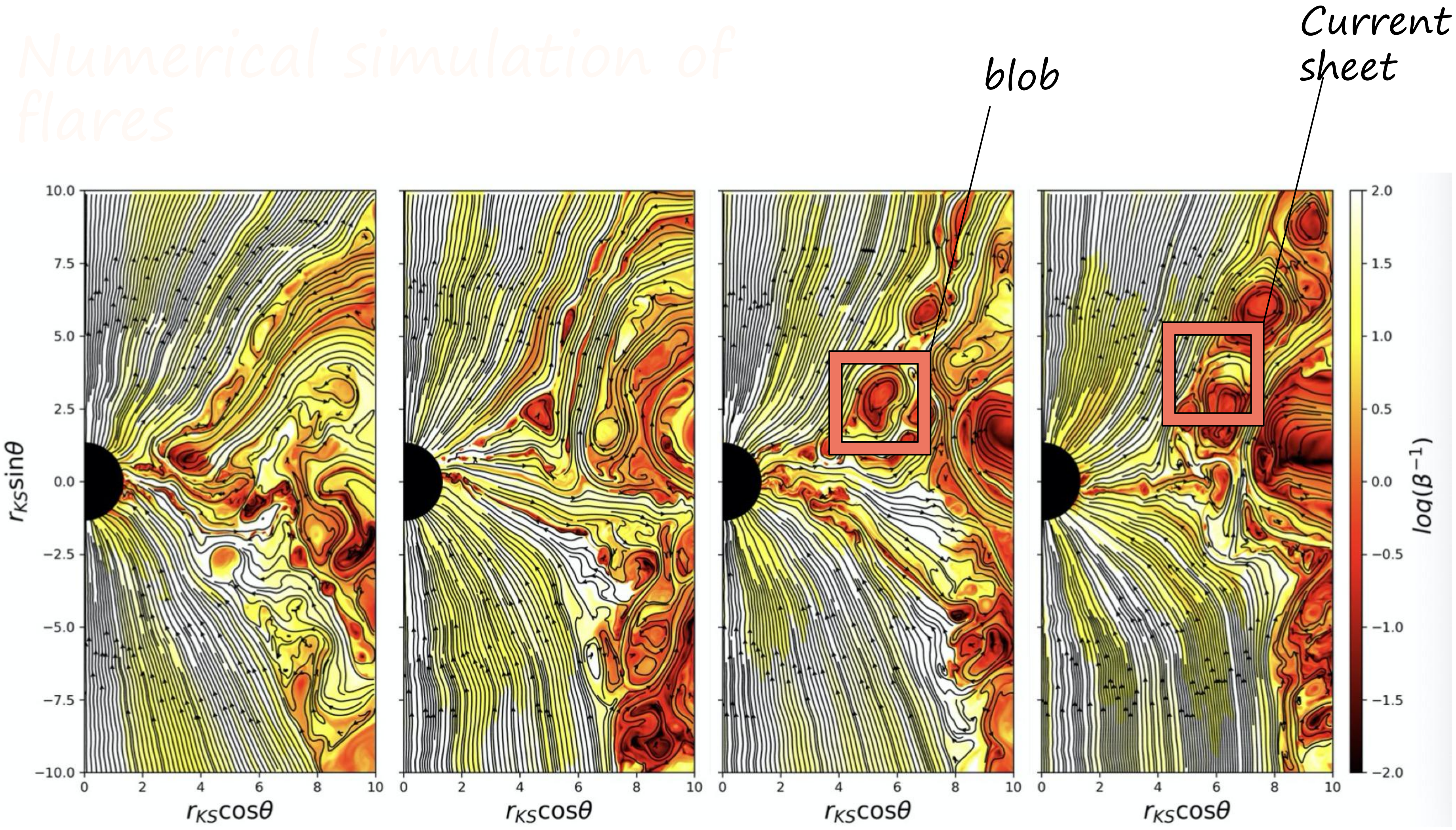

Ripperda et al (2020) perform axisymmetric general-relativistic resistive magnetohydrodynamics(GRMHD) simulations to model magnetic reconnection and associated plasmoid formation in a wide range of accretion flows.

Magnetic Reconnection Model

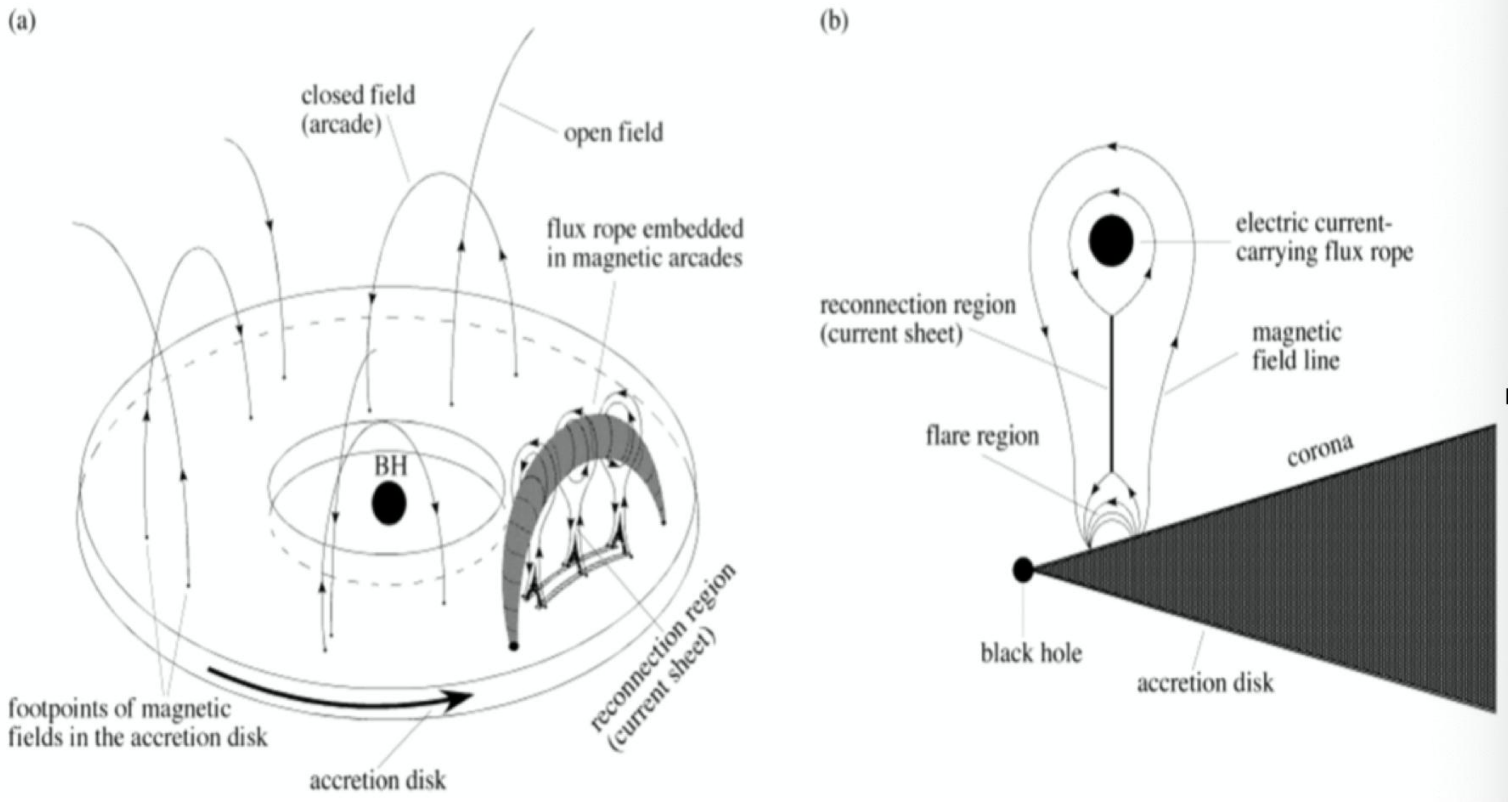

Yuan F., Lin J., Wu K., Ho L. C., 2009, MNRAS, 395, 2183

Plasmoid merger during the magnetic reconnection

Numerical Model

$$\partial_t \rho = -\nabla \cdot (\rho \mathbf{v}) \qquad (1)$$

$$\partial_t \mathbf{B} = -\nabla \times (\mathbf{v} \times \mathbf{B} - \eta \nabla \times \mathbf{B}) \qquad (2)$$

$$\partial_t (\rho \mathbf{v}) = -\nabla \cdot [\rho \mathbf{v}\mathbf{v} + (p + \frac{1}{2\mu_0} |\mathbf{B}|^2)\mathbf{I}] + \nabla \cdot [\frac{1}{\mu_0} \mathbf{B}\mathbf{B}] + \rho \mathbf{g} \qquad (3)$$

$$\partial_t e = -\nabla \cdot [(e + p + \frac{1}{2\mu_0} |\mathbf{B}|^2)\mathbf{v}] + \nabla \cdot [\frac{1}{\mu_0} (\mathbf{v} \cdot \mathbf{B})\mathbf{B}] + \nabla \cdot [\frac{\eta}{\mu_0} \mathbf{B} \times (\nabla \times \mathbf{B})] - \nabla \cdot \mathbf{F}_C + \rho \mathbf{g} \cdot \mathbf{v} \qquad (4)$$

$$e = \frac{p}{\Gamma_0 - 1} + \frac{1}{2} \rho |\mathbf{v}|^2 + \frac{1}{2\mu_0} |\mathbf{B}|^2 \qquad (5)$$

$$p = \frac{2\rho}{m_i} k_B T \qquad (6)$$

Numerical Model

Bx=-0.6b_0 By=-0.8b_0 b_0=0.0016T

density $$\rho = \rho_0 \times exp\left(-\frac{x^2}{{H_0}^2}\right)$$

pressure $$P_0 = \frac{2\rho_0 k_B T_0}{m_i}$$

Thermal energy density $$Et_0 = \frac{P_0}{\gamma - 1},$$

$$\rho\nabla\Phi = -\nabla P.$$

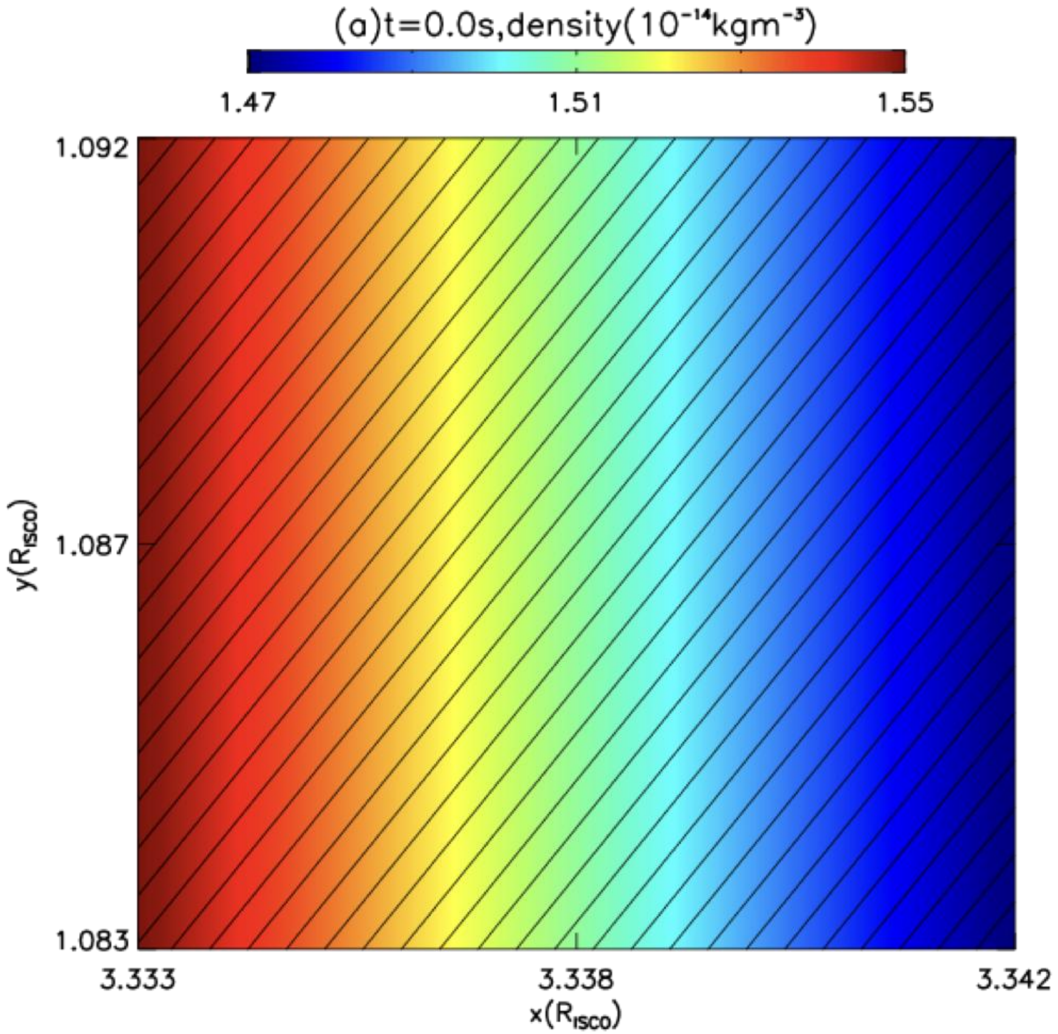

Region: 3.0e8 m*3.0e8 m

Numerical Model

Y low:

$$b_{xb} = -0.6b_0 + \frac{100L_0(y-y_0)b_1 f}{[(x-x_0)^2+(y-y_0)^2]}\left[\tanh\left(\frac{x-170L_0}{\lambda}\right) - \tanh\left(\frac{x-230L_0}{\lambda}\right)\right],$$

$$b_{yb} = -0.8b_0 - \frac{100L_0(x-x_0)b_1 f}{[(x-x_0)^2+(y-y_0)^2]}\left[\tanh\left(\frac{x-170L_0}{\lambda}\right) - \tanh\left(\frac{x-230L_0}{\lambda}\right)\right],$$

X low : outflow
X upper :outflow
Y upper: outflow

where $t \le t_1$ for $f = t/t_1$ and $t \ge t_1$ for $f = 1$

Case	g_x ($\mathrm{m\,s^{-2}}$)	R_{in} (R_s)	ρ_0 (kgm^{-3})	$T_0(K)$	H_0	plasma-β	σ	η
Case I	-47087.009	$10R_s$	5.2×10^{-14}	3.0×10^{10}	$7.5R_s$	2.18	0.0025	η_{TD}
Case II	-47087.009	$10R_s$	5.2×10^{-14}	3.0×10^{10}	$7.5R_s$	2.18	0.0025	η_C

Numerical result

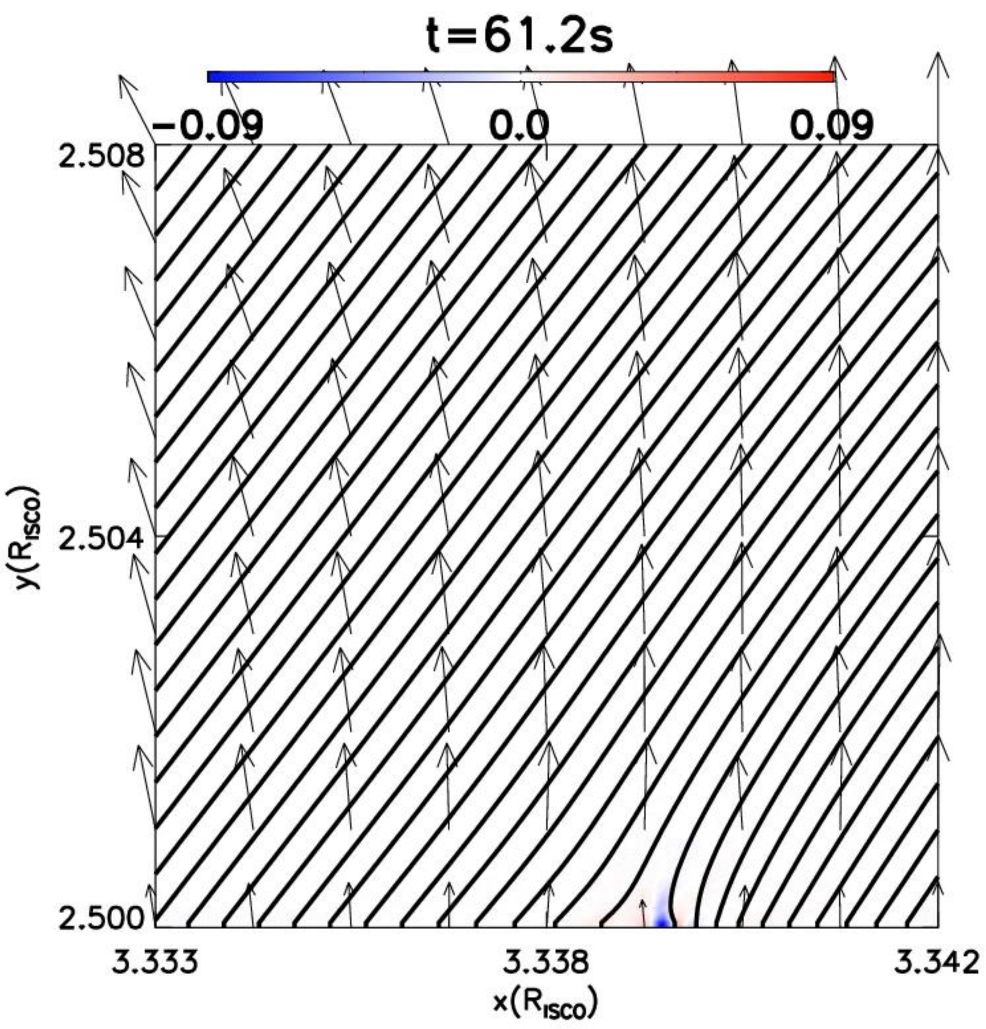

Plasmoid merger with the temperature-dependent diffusion

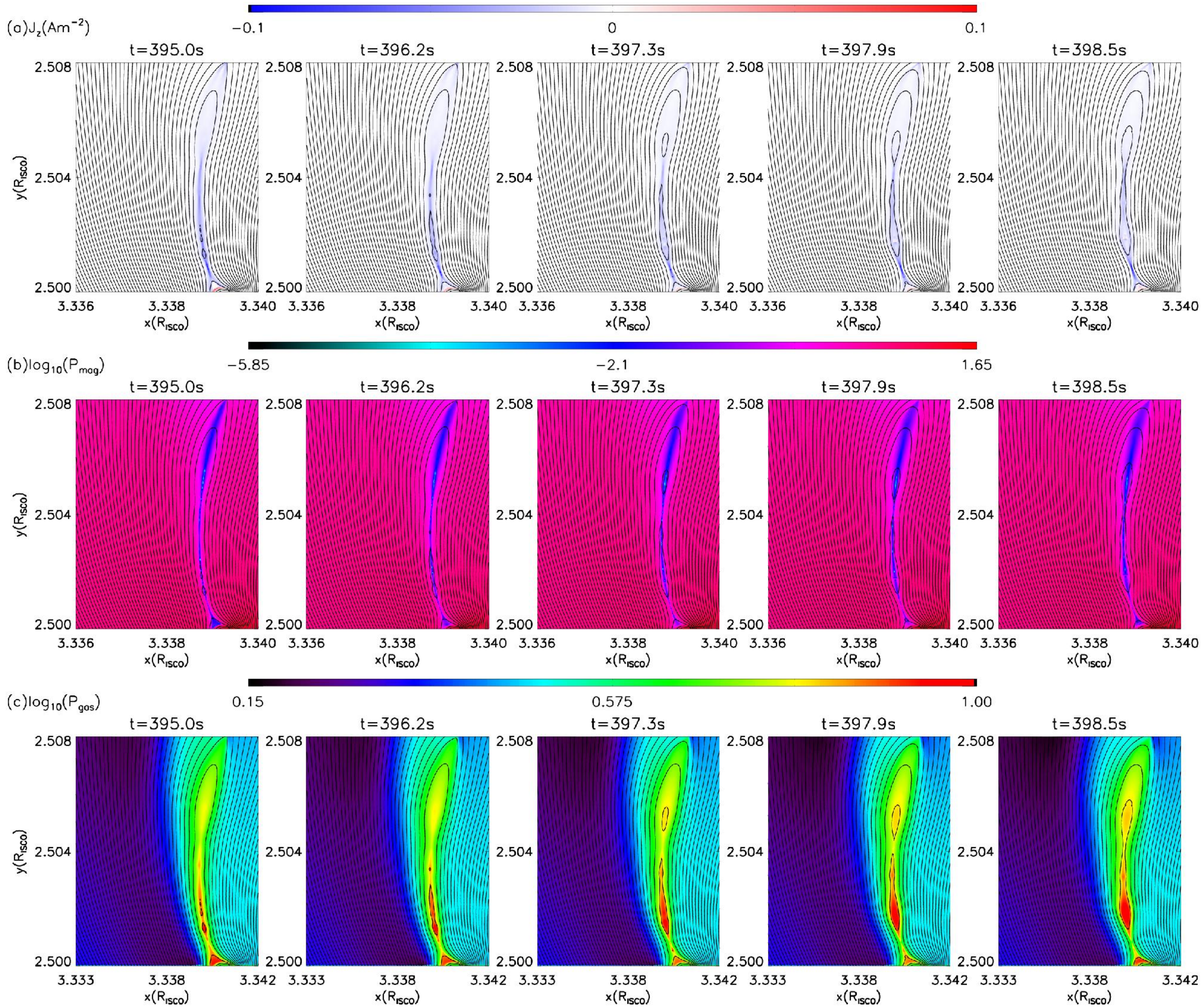

(a)$J_z(Am^{-2})$
−0.1
0
0.1
(b)$log_{10}(P_{mag})$
−5.85
−2.1
1.65
(c)$log_{10}(P_{gas})$
0.15
0.575
1.00
t=395.0s
t=396.2s
t=397.3s
t=397.9s
t=398.5s
$y(R_{ISCO})$
$x(R_{ISCO})$
2.508
2.504
2.500
3.336
3.338
3.340
3.333
3.338
3.342

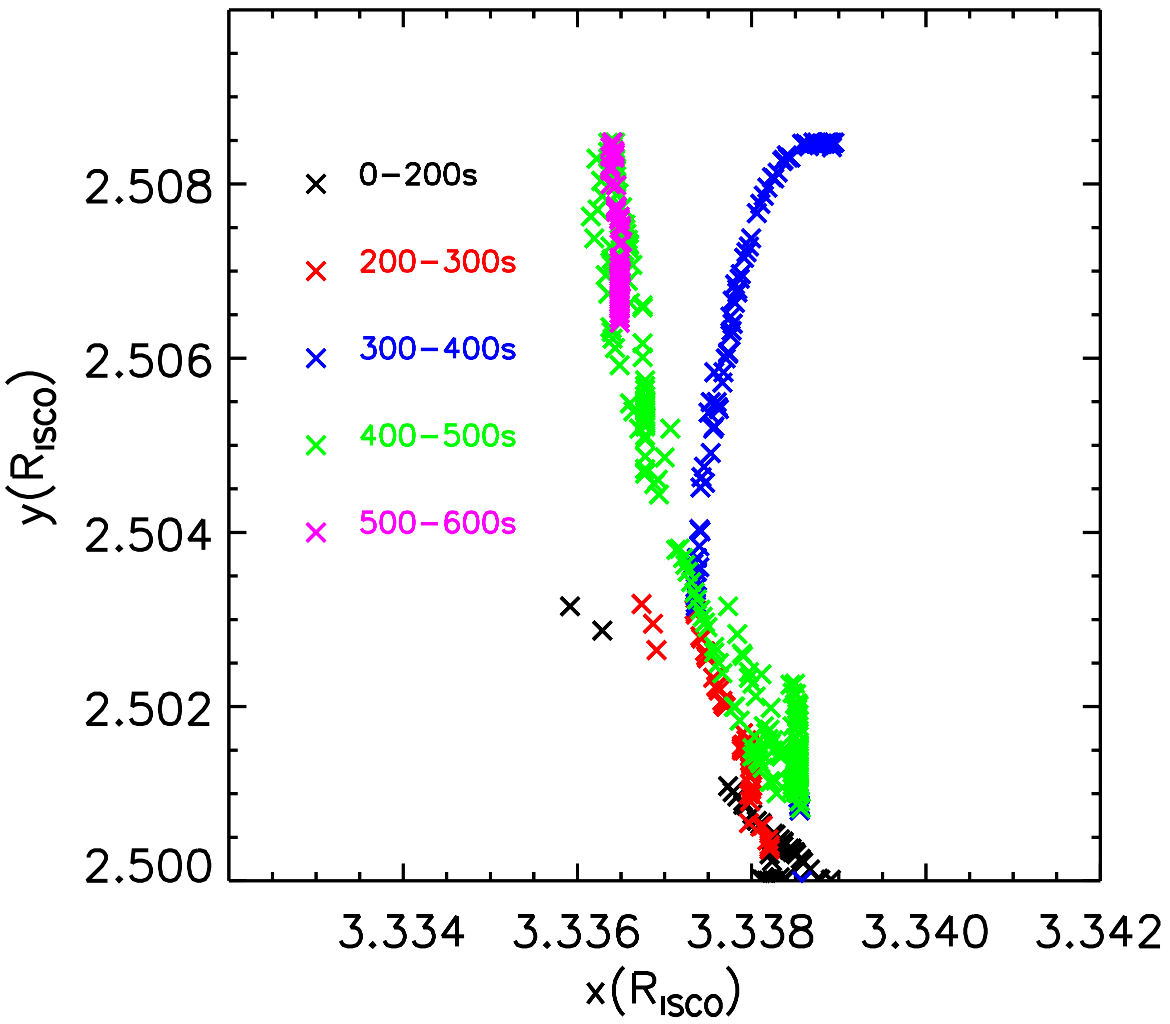

Distributions of the main X-point during the magnetic reconnection change with the time

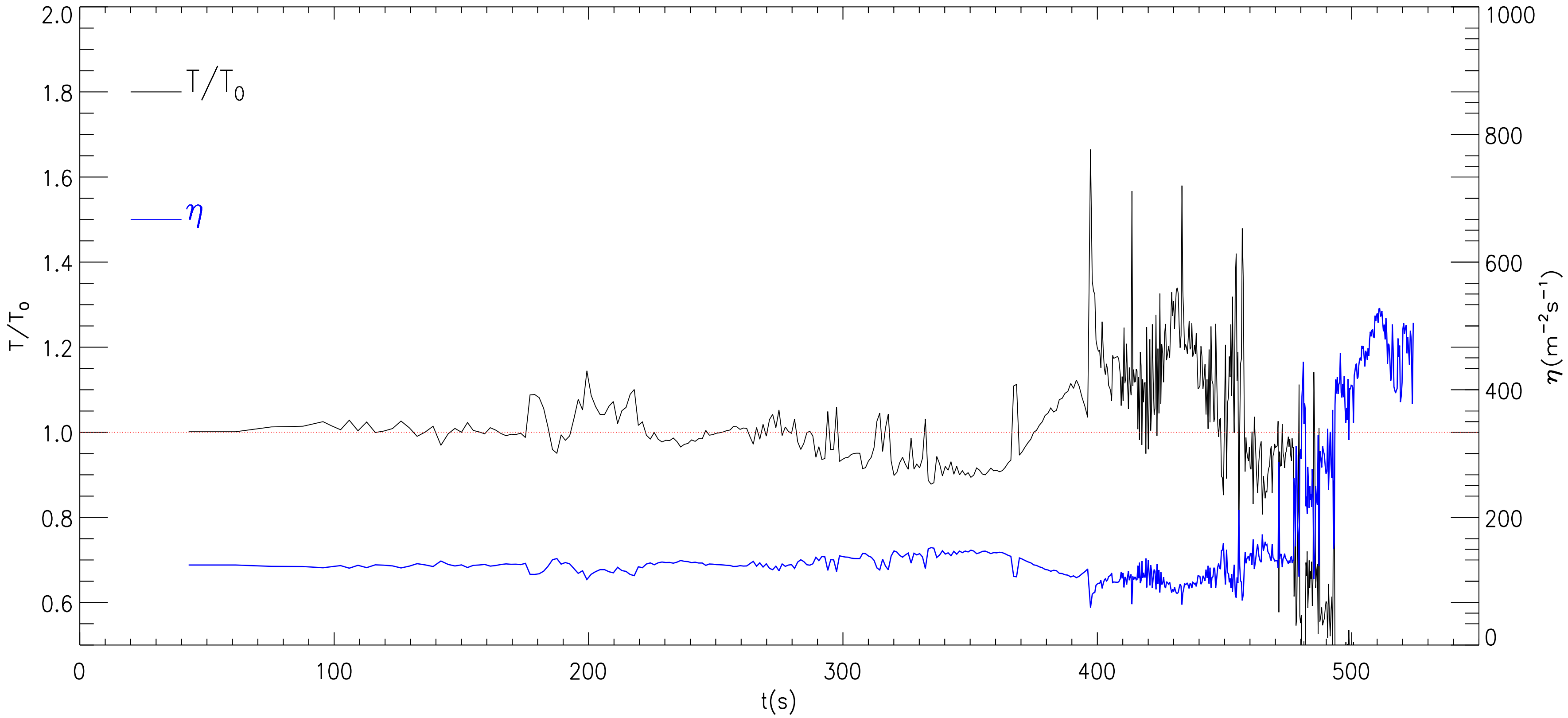

$$\eta = 10^8 \left(T_0/T\right)^{3/2} + 10^9 \left[1 - \tanh\left(\frac{y - 2L_0}{0.2L_0}\right)\right] (\mathrm{m^2 s^{-1}}).$$

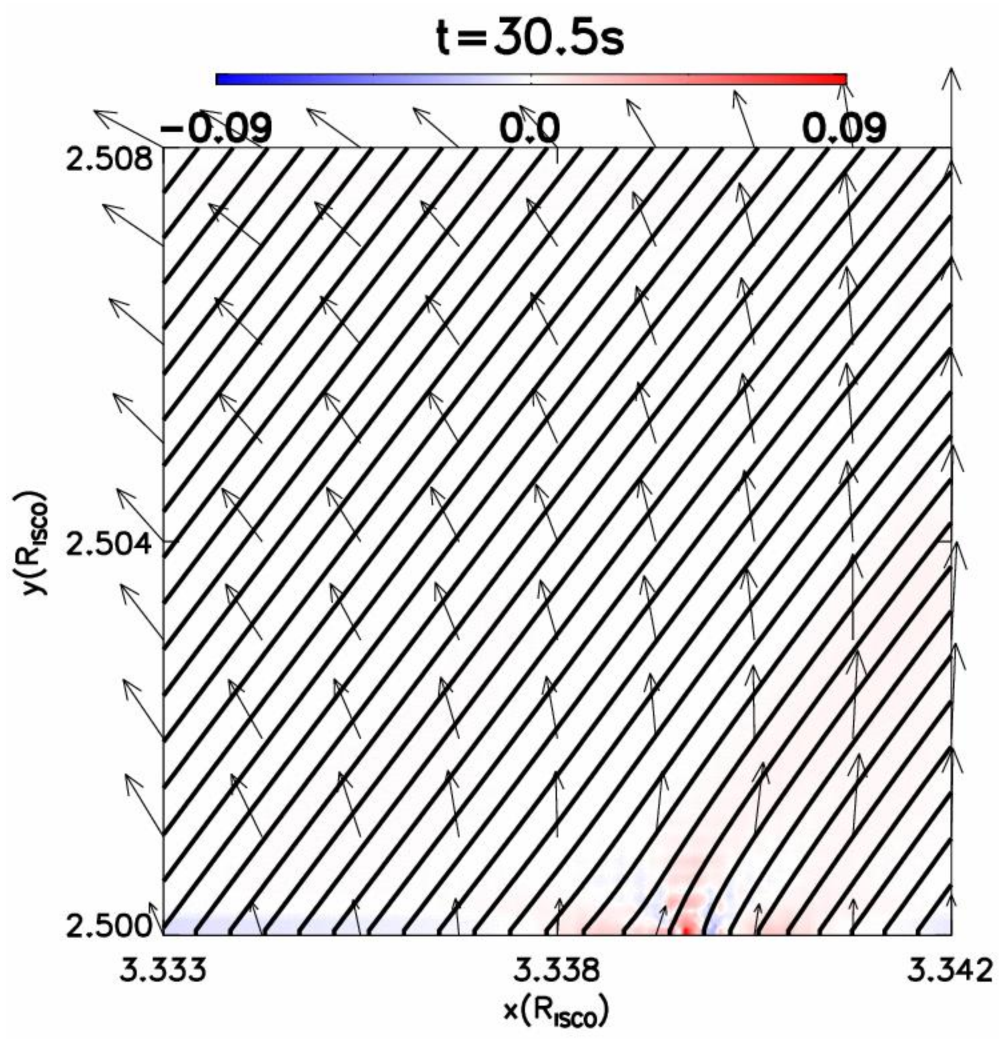

Plasmoid merger with the constant diffusition
Current density

η_{TD}

η_{C}

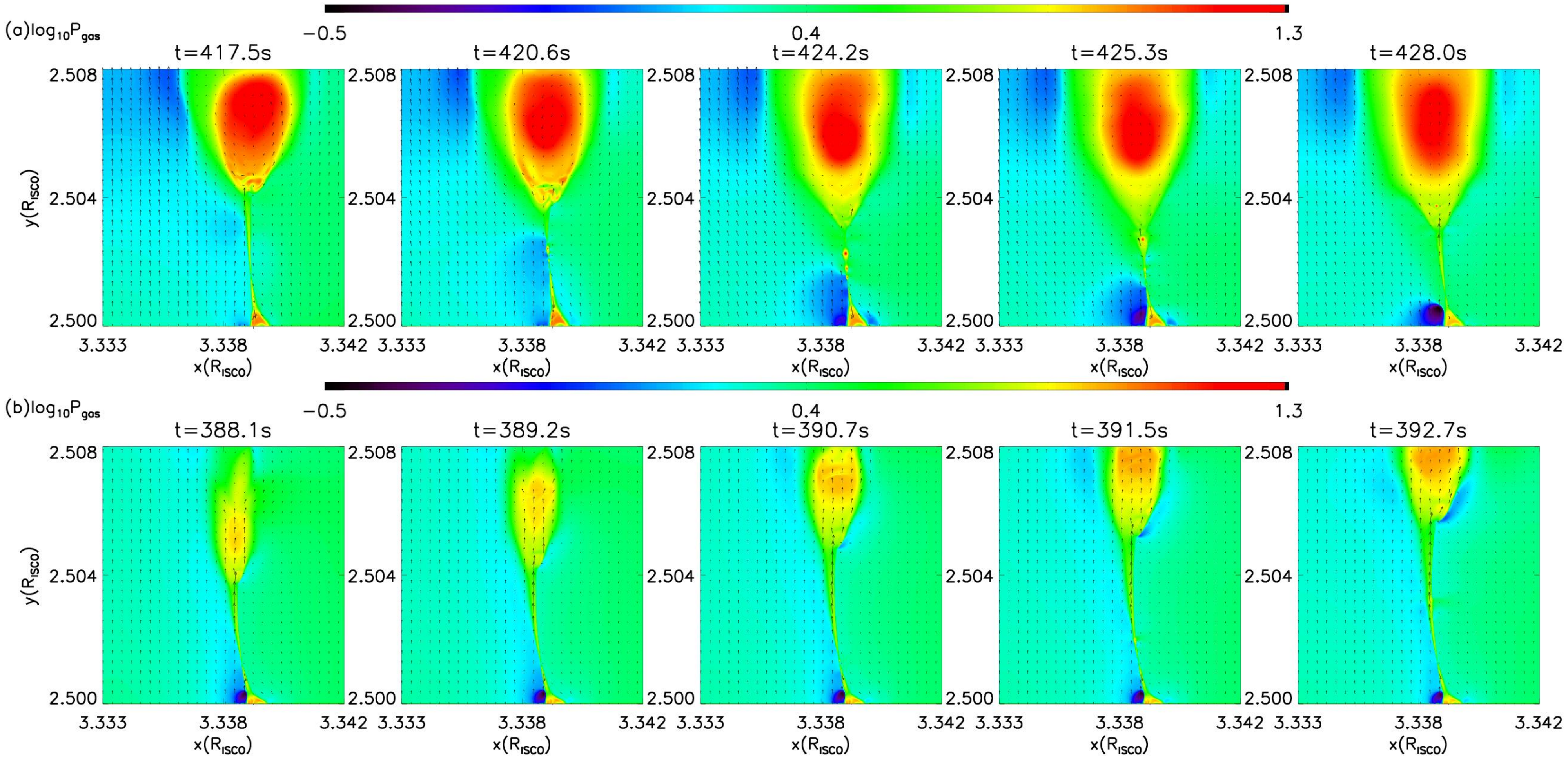

Gas pressure with the velocity vector

温度主
导电阻

常数
电阻

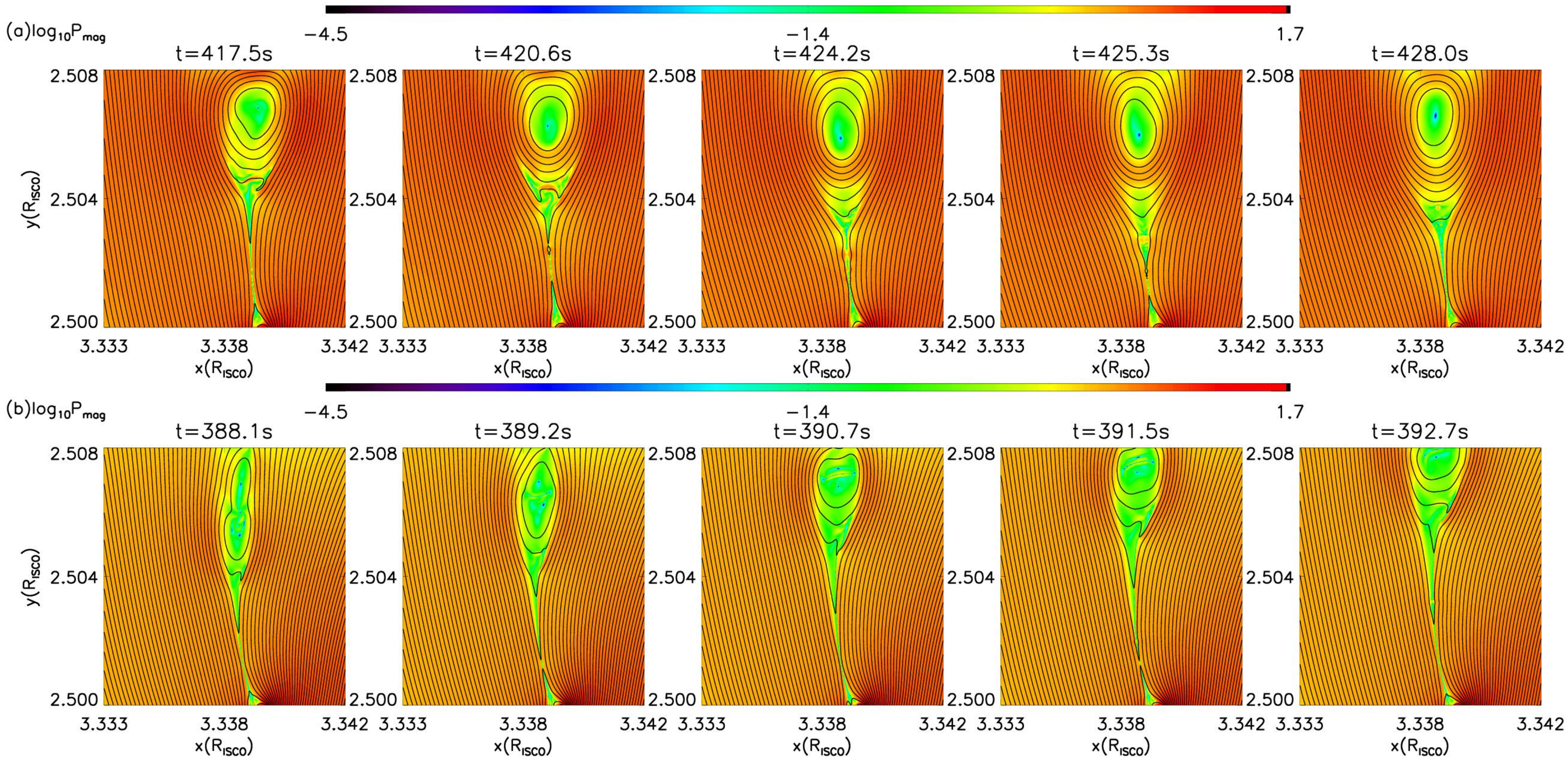

磁压和磁力线分布

Shock wave during the magnetic reconnection

Numerical Model

$$\phi = -GM/(\sqrt{x^2+y^2} - R_s),$$

$$\rho(x,y) = \rho_0 \exp(-(x^2+y^2)/H_0^2),$$

$$T_0 = 2 \times 10^{10}\ \mathrm{K},$$

$$\rho(R_{in}, H_0) = 1.04 \times 10^{-13}\ \mathrm{kg\ m^{-3}}$$

$$H_0 = 5R_s,$$

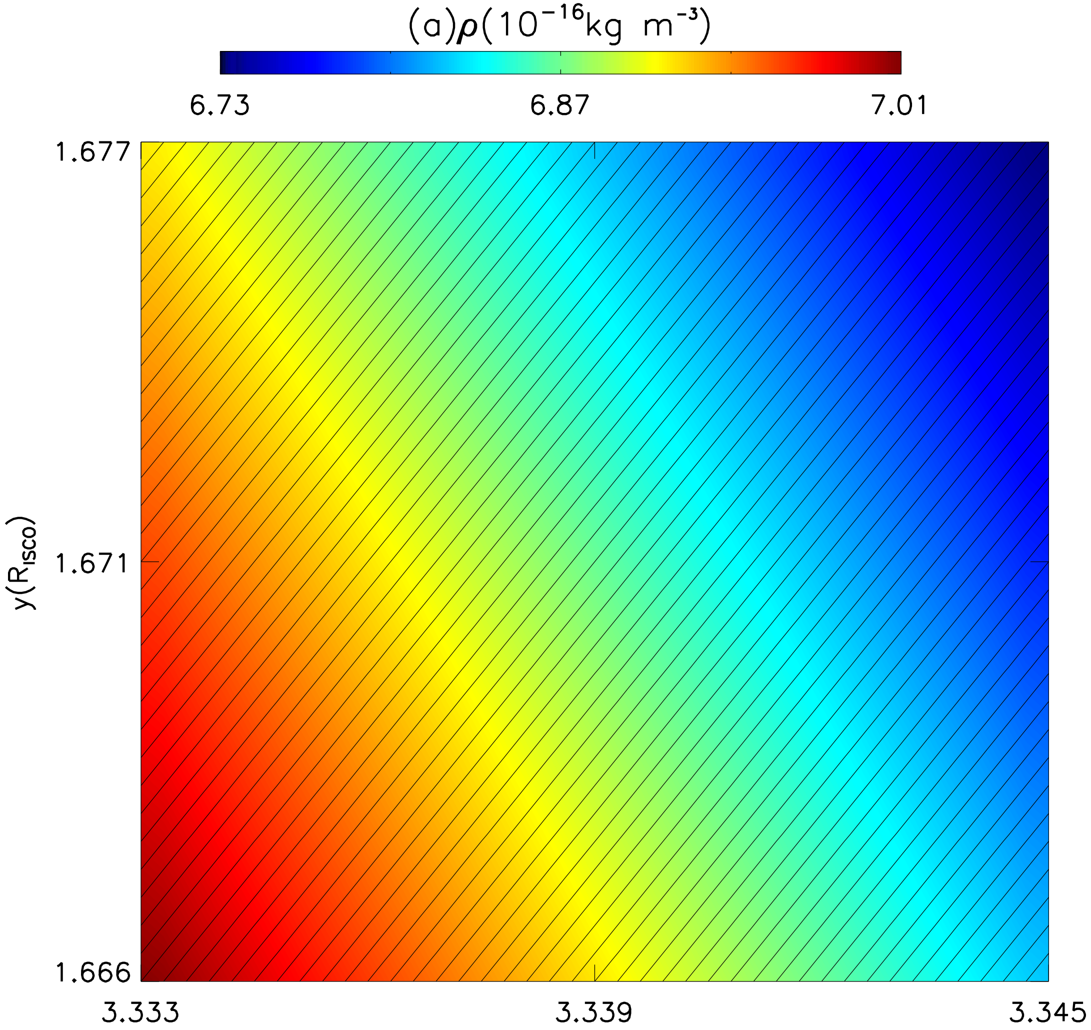

$$b_{xb} = -0.6b_0 + \frac{100L_0(y-y_0)b_1 f}{[(x-x_0)^2+(y-y_0)^2]}\left\{\left[\tanh\left(\frac{x-170L_0-R_{in}}{\lambda}\right) - \tanh\left(\frac{x-330L_0-R_{in}}{\lambda}\right)\right]\right\},$$

$$b_{yb} = -0.8b_0 - \frac{100L_0(x-x_0)b_1 f}{[(x-x_0)^2+(y-y_0)^2]}\left\{\left[\tanh\left(\frac{x-170L_0-R_{in}}{\lambda}\right) - \tanh\left(\frac{x-330L_0-R_{in}}{\lambda}\right)\right]\right\},$$

Numerical result

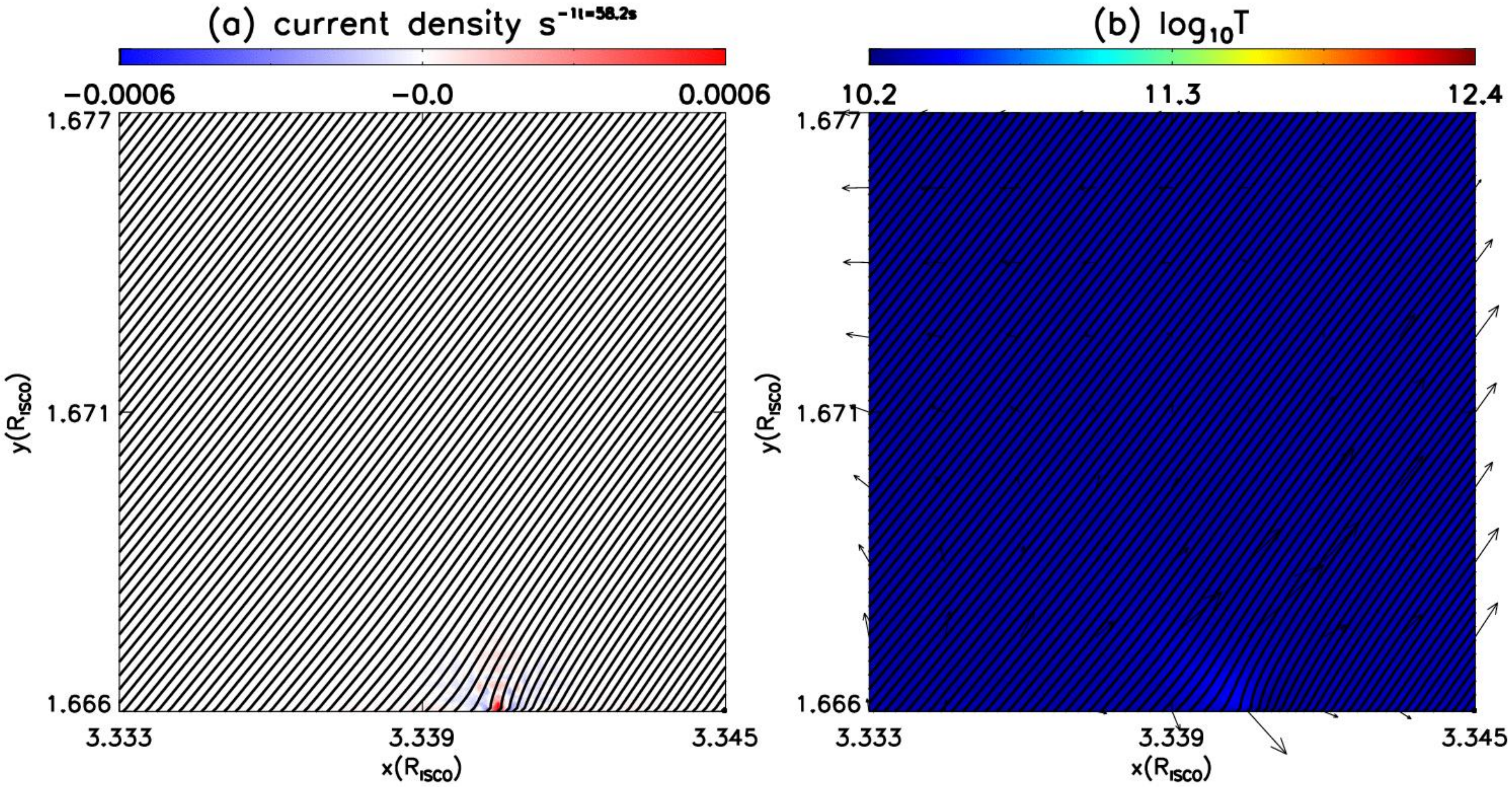

Numerical result

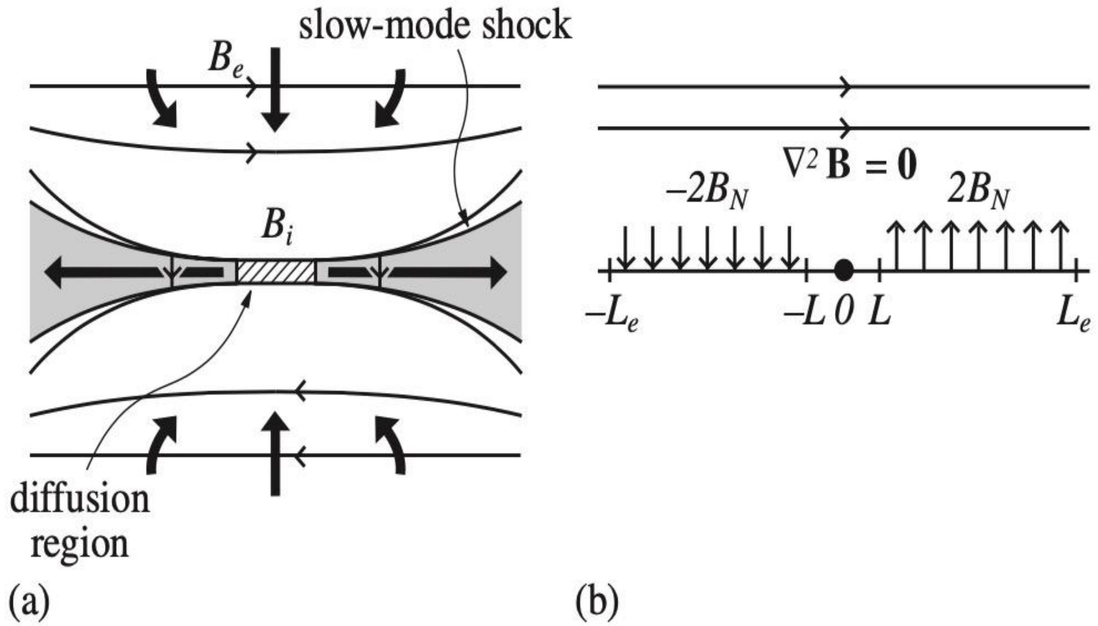

Petschek model

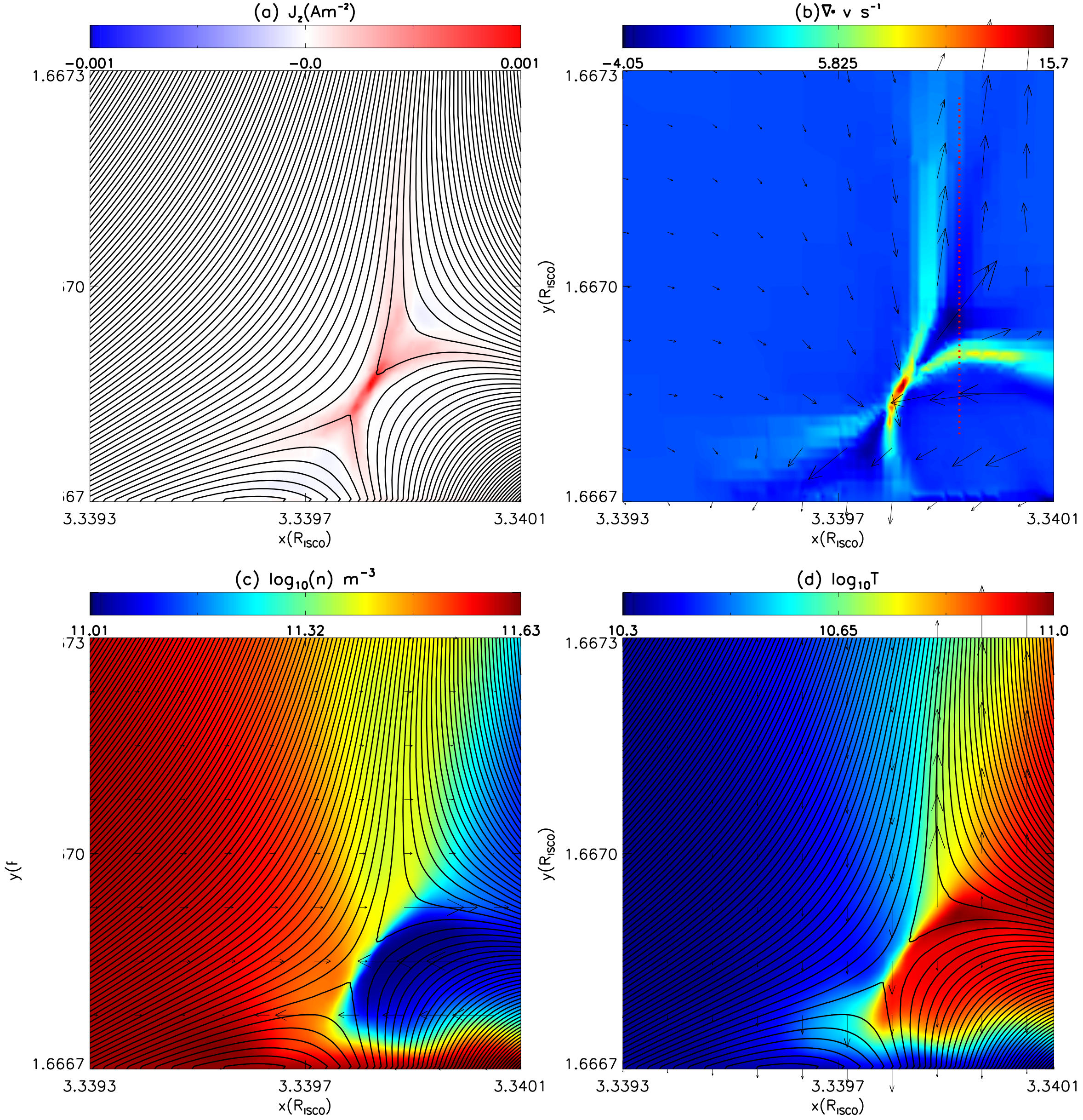

Current density, Velocity divergence, Number density and Temperature

Numerical res

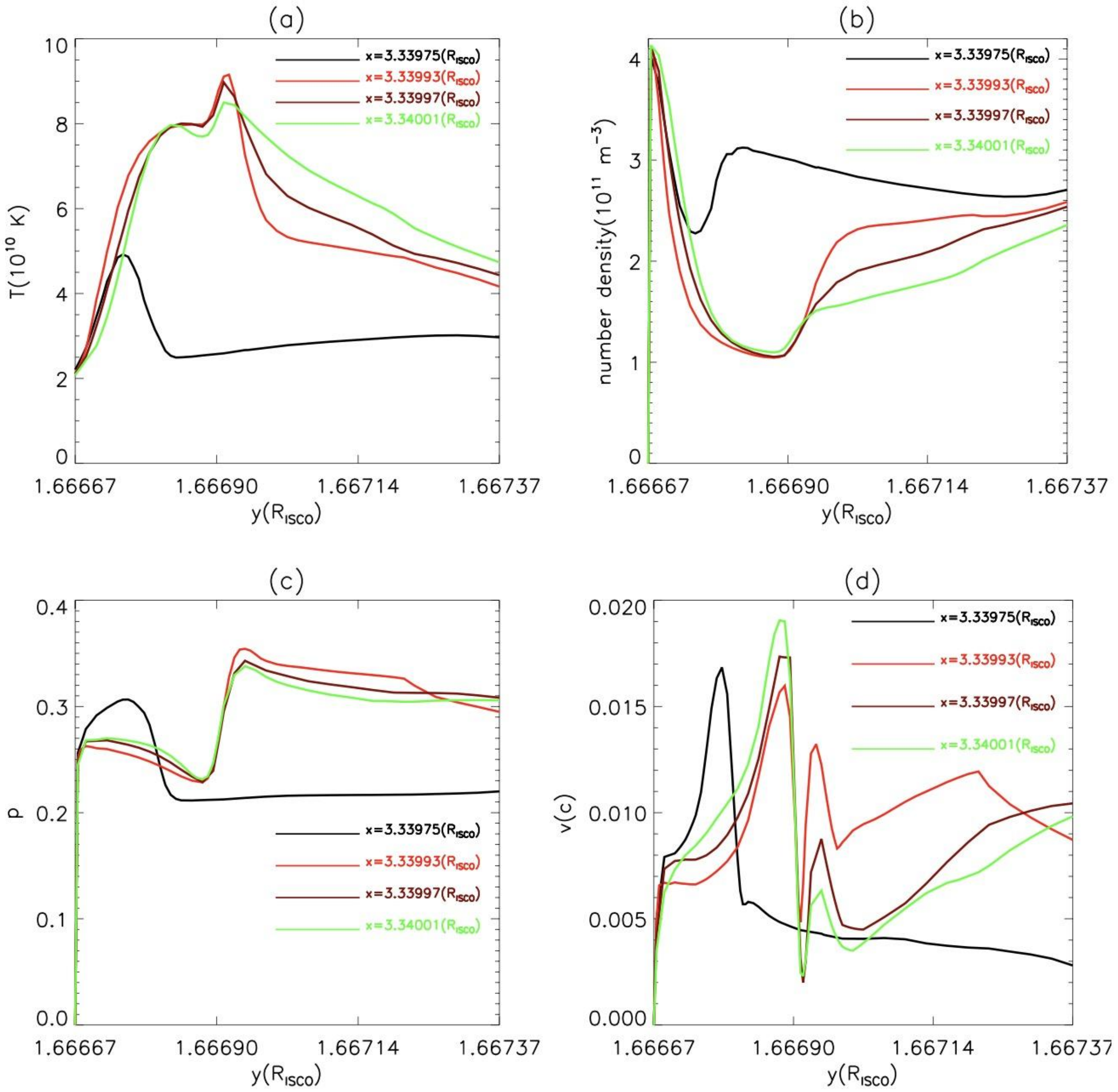

Physical quantity distribution vary along y-direction at four different x location at t=194.39s

Numerical resu

$$B_{n1} = B_{n2}$$

$$\rho_1 v_{n1} = \rho_2 v_{n2}$$

$$\rho_1 v_{n1}^2 + P_1 + \frac{B_{t1}^2}{2\mu_0} = \rho_2 v_{n2}^2 + P_2 + \frac{B_{t2}^2}{2\mu_0}$$

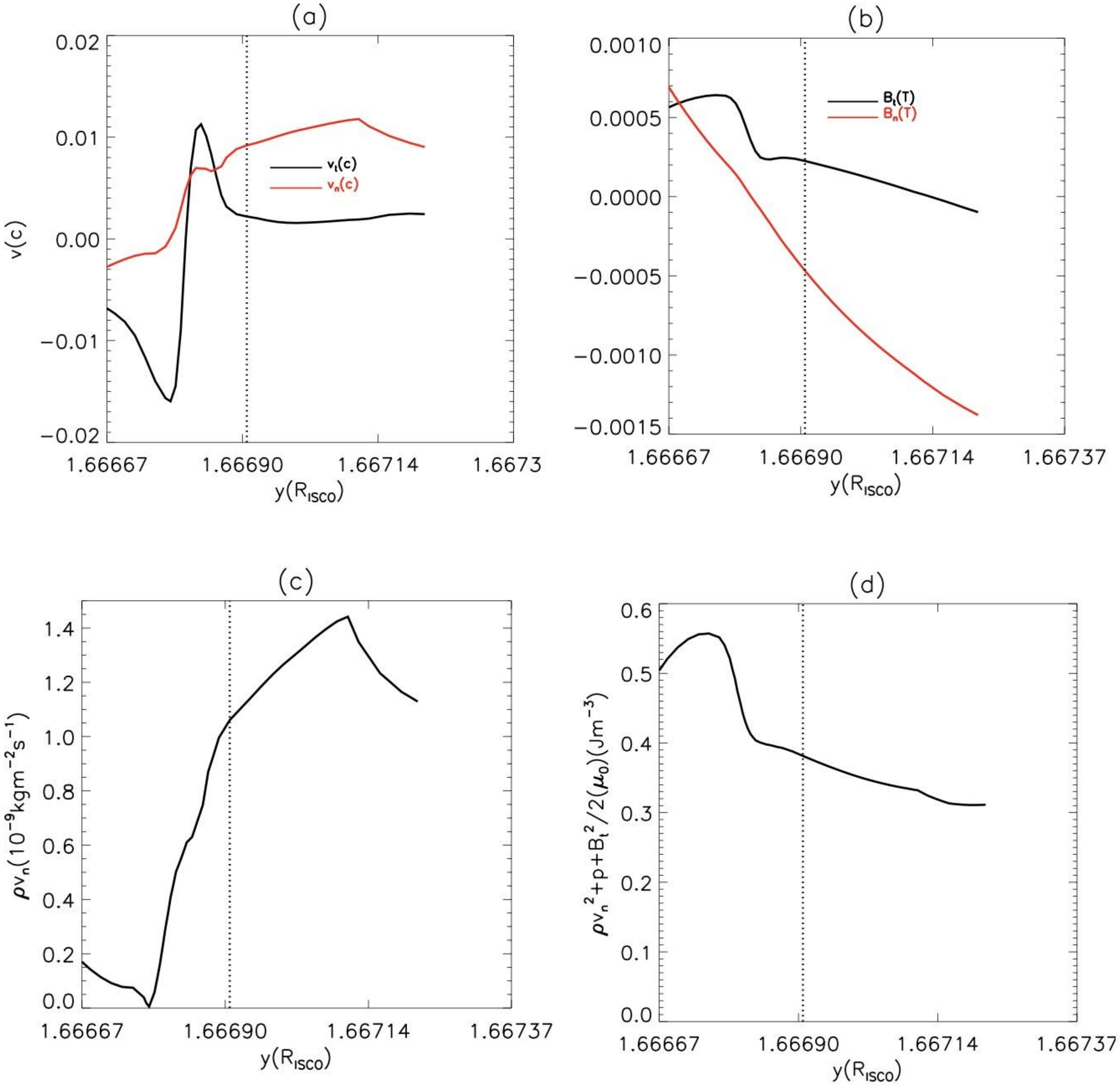

Conclusion

- During the magnetic reconnection, the Alfven Mach number in some area around the plasmoid is larger than 1, which leads to the super-Aflvenic motions occurring around the plasmoid, it is large enough to trigger the formation and ejection of the plasmoid.
- Under the initial condition of the temperature-dependent magnetic diffusivity η_{TD}, the higher temperature cause the lower magnetic diffusivity. The principal X-point has a very high magnetic diffusivity. A huge plasmoid can form due to the combined effects of the new principal X-point and the old principal X-point.
- During the huge plasmoid forms, the temperature-dependent magnetic diffusivity leads the plasmoid oscillate and deform for a long time then be pulled out by the magnetic reconnection, but under the constant diffusivity, the huge plasmoid forms early and then be pulled out without deformation.
- Shock waves mainly heat the plasma in the outflow region

Thank you